Plant Molecular Biology
https://doi.org/10.1007/s11103-021-01215-y

Editing of the starch branching enzyme gene *SBE2* generates high-amylose storage roots in cassava

Shu Luo[1,2] · Qiuxiang Ma[1] · Yingying Zhong[1,3] · Jianling Jing[1] · Zusheng Wei[4] · Wenzhi Zhou[1,3] · Xinlu Lu[1] · Yinong Tian[4] · Peng Zhang[1,2]

Received: 12 June 2021 / Accepted: 3 November 2021

Abstract

Key message **The production of high-amylose cassava through CRISPR/Cas9-mediated mutagenesis of thestarch branching enzyme gene SBE2 was firstly achieved.**

Abstract High-amylose cassava (*Manihot esculenta* Crantz) is desirable for starch industrial applications and production of healthier processed food for human consumption. In this study, we report the production of high-amylose cassava through CRISPR/Cas9-mediated mutagenesis of the starch branching enzyme 2 (SBE2). Mutations in two targeted exons of *SBE2* were identified in all regenerated plants; these mutations, which included nucleotide insertions, and short or long deletions in the *SBE2* gene, were classified into eight mutant lines. Three mutants, M6, M7 and M8, with long fragment deletions in the second exon of *SBE2* showed no accumulation of SBE2 protein. After harvest from the field, significantly higher amylose (up to 56% in apparent amylose content) and resistant starch (up to 35%) was observed in these mutants compared with the wild type, leading to darker blue coloration of starch granules after quick iodine staining and altered starch viscosity with a higher pasting temperature and peak time. Further ^{1}H-NMR analysis revealed a significant reduction in the degree of starch branching, together with fewer short chains (degree of polymerization [DP] 15–25) and more long chains (DP>25 and especially DP>40) of amylopectin, which indicates that cassava SBE2 catalyzes short chain formation during amylopectin biosynthesis. Transition from A- to B-type crystallinity was also detected in the starches. Our study showed that CRISPR/Cas9-mediated mutagenesis of starch biosynthetic genes in cassava is an effective approach for generating novel varieties with valuable starch properties for food and industrial applications.

Keywords Cassava · Genome editing · High amylose · Starch branching enzymes · Starch property

Introduction

Cassava (*Manihot esculenta* Crantz, 2n=36) is a starchy root crop feeding more than 800 million people in tropical regions (Sayre et al. 2011). It is ranked as the world's fourth most important staple food after rice, wheat, and maize (FAO, 2019). Fresh cassava storage roots have high starch content (up to 32%) and are traditionally processed into various foods in sub-Sahara Africa and Latin America. Dehydrated cassava chips are mainly commercialized as bioindustrial feedstock for bioethanol, modified starch, and biomaterial, especially in Southeast Asian countries (FAO, 2019). Cassava starch, including modified starch, has a variety of properties that make it suitable for use as, for example, a texturizer, additive, stabilizer, and thickener, in many industrial processes (Breuninger et al. 2009). In particular, cassava starch, which has a high content of

✉ Qiuxiang Ma
qxma@cemps.ac.cn

✉ Peng Zhang
zhangpeng@cemps.ac.cn

1 National Key Laboratory of Plant Molecular Genetics, CAS Center for Excellence in Molecular Plant Sciences, Chinese Academy of Sciences, Shanghai 200032, China

2 University of Chinese Academy of Sciences, Beijing, China

3 Shanghai Sanshu Biotechnology Co., LTD, Shanghai 201210, China

4 Guangxi Subtropical Crops Research Institute, Nanning 530001, China

Published online: 18 November 2021

amylose, is beneficial for patients who are obese and diabetic and also for new industrial applications such as biodegradable plastics (Li et al. 2019). To meet the demand for cassava starch with desirable functional properties, genetic improvement of cassava has drawn more attention by breeders over the past decade, especially efforts to increase the ratio of amylose to amylopectin (Ceballos et al. 2020; Zhou et al. 2020). Nevertheless, due to its genome complexity, monoecious and self-incompatibility, and sporadic flowering and less seed (Ceballos et al. 2010; Pootakham et al. 2014), cassava starch improvement by traditional breeding is difficult and genome editing is in demand (Bull et al. 2018).

Cassava native starch, like most starch, is mainly composed of amylose (contents usually ranging from 20 to 30%) and amylopectin (contents ranging from 70 to 80%). Granule bound starch synthase (GBSS), which is chaperoned by PTST1 (Seung et al. 2015), is mainly responsible for long-chain glucan amylose biosynthesis, which occurs in amyloplasts or chloroplasts of plant cells. In cassava, *GBSS* gene mutation by heavy ion irradiation, down-regulation by RNAi, or editing by CRISPR/Cas9 leads to a waxy starch phenotype (Ceballos et al. 2007; Zhao et al. 2011; Bull et al. 2018). The synthesis of highly-branched amylopectin requires series of synthases, including soluble starch synthase (SS) and a starch branching enzyme (BE) and debranching enzyme (DBE). Phylogenetic and evolutionary analysis of the soluble SSs in cassava has shown that a point mutation under positive selection contributed to the evolution of the *MeSSI* and *MeGBSSI* genes (Yang et al. 2013). Down-regulation of cassava *SSII* expression by RNAi increased amylose content up to 33% and the amount of resistant starch by interrupting protein interactions among the starch biosynthetic protein complexes (He et al. 2020). Down-regulation of *SBE2*, but not *SBE1*, expression in cassava led to more than 50% higher amylose accumulation (Zhou et al. 2020), suggesting that SBE2 was a suitable target for genome editing to generate high-amylose cassava.

The development of the CRISPR/Cas system for site-specific editing of plant genomes has facilitated mutagenesis of target genes for desirable traits in crops and paved the way for crop breeders to produce transgene-free improved varieties through genetic segregation by selfing and crossing (Chen et al. 2019). This technology has been used to modify starch quality by targeting starch biosynthesis genes or their promoters in several important crops including rice, wheat, maize, potato, and sweet potato (Andersson et al. 2017; Sun et al. 2017; Dong et al. 2019; Johansen et al. 2019; Tuncel et al. 2019; Wang et al. 2019; Li et al. 2020; Zeng et al. 2020; Zhao et al. 2021). In cassava, CRISPR/Cas9-mediated mutations in *GBSSI* and *PTST1* result in the reduction of amylose content in storage root starch (Bull et al. 2018). Similarly, *IbGBSSI*- or *IbSBEII*-knockout sweet potato lines showed altered amylose percentages in their storage roots (Wang et al. 2019). CRISPR/Cas9-mediated mutagenesis of starch biosynthetic genes (*GBSS*, *SBE1*, and/or *SBE2*) in potato also gave rise to a range of tuber starch phenotypes (Carciofi et al. 2012; Andersson et al. 2017; Johansen et al. 2019; Tuncel et al. 2019; Zhao et al. 2021).

To develop high-amylose cassava, there is a need to generate *SBE2*-edited cassava using the CRISPR/Cas9-system. In this study, mutagenesis of *SBE2* in cassava was achieved using the dual-sgRNA CRISPR/Cas9 system. Our results showed that cassava plants with a long fragment deletion in *SBE2* accumulated no functional SBE2 protein, resulting in a high-amylose starch phenotype with altered starch physico-chemical properties in the storage roots.

Materials and methods

Phylogeny and conserved motif analysis of SBEs

Genomic and amino acid sequences of SBEs from different plants species were obtained from NCBI GenBank. Multiple amino acid sequences were aligned by ClustalW and phylogenetic tree was constructed in MEGA 7.0 with the neighbor-joining method. The bootstrap values were obtained with 1000 replications. Gene structure and conserved motif analysis were performed and modified with GSDS 2.0 and MEME web server 5.3.1, respectively (Bailey et al. 2009). Annotations of conserved motifs were referred to SMART database in PDBsum format.

CRISPR/Cas9-based vector construction and production of *SBE2* cassava mutants

The backbone of the CRISPR/Cas9 vector used in the study was previously reported (Mao et al. 2013; Cong et al. 2013). The target sequence harboring the NGG nucleotides was searched using the cassava genome information based on the Phytozome database (https://phytozome-next.jgi.doe.gov/info/Mesculenta_v6_1), and two specific sgRNAs were designed to recognize the second and fifth exons in cassava *SBE2* gDNA (Fig. 1). *SBE2 sgRNA1* (5′-TCTAAAAGA GTCCTTCCTGATGGTCGGATT-3′) and *SBE2 sgRNA2* (5′-AATAACTTATAGAGAGTGGGCACCAGGAGC-3′) were both driven by U6-26 promoter from *Arabidopsis* (Mao et al. 2013). *SpCas9* was driven by the promoter of *Arabidopsis UBQ1* gene (Mao et al. 2013; Cong et al. 2013). The backbone of the *SpCas9* and sgRNA expression cassettes was digested by *Eco*R I and *Hin*d III, and ligated into the pCAMBIA1301 binary vector, which harbors the hygromycin phosphotransferase gene. The constructed vector was introduced into *Agrobacterium tumefaciens* LBA4404, and the friable embryogenic callus of African cassava cultivar

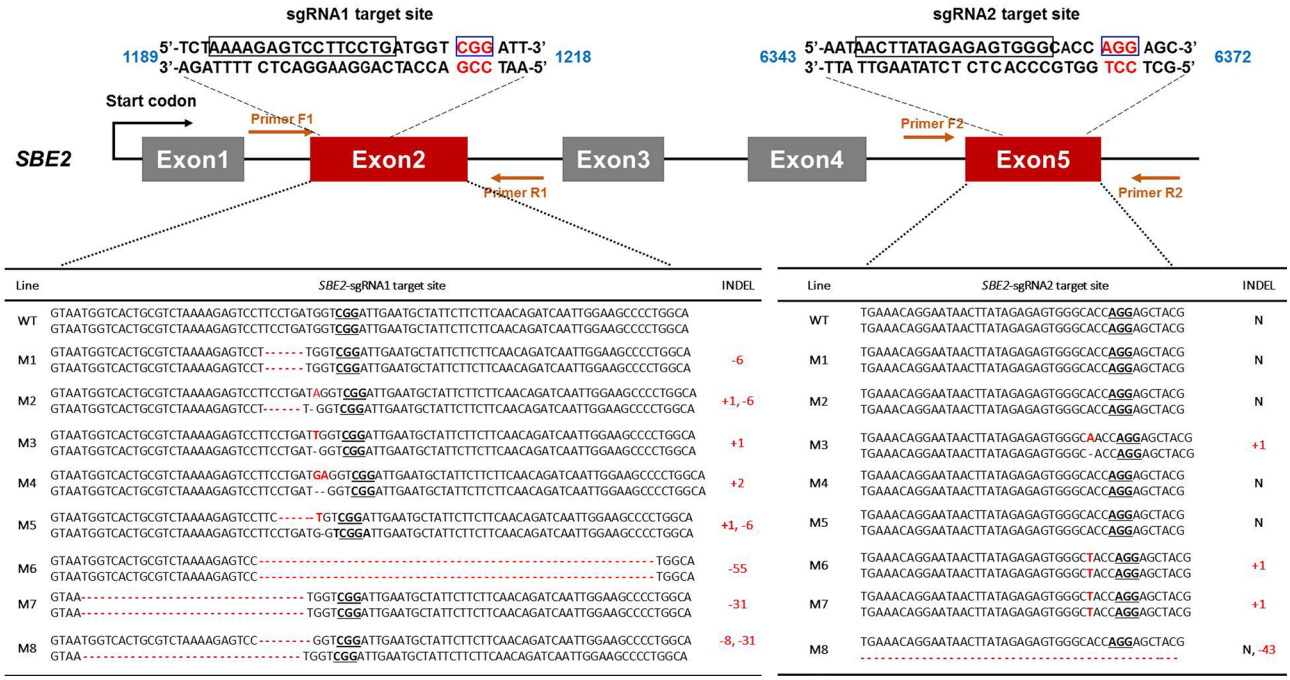

Fig. 1 Mutations in the cassava *SBE2* genome DNA sequence. The sgRNAs targeting the second and fifth exons of *SBE2* genomic DNA are illustrated. Eight mutant lines of INDELs were classified by sequencing PCR amplicons. Underlined bold fonts indicate the PAM; red dashes indicate deletions; red font indicates insertions; numbers in the right panel indicate the size of the mutation ("N" represents no mutation)

TMS60444, which is frequently used for genetic transformation, was used to generate transgenic plants as described previously (Zhang et al. 2000).

The WT and transgenic cassava plants were propagated as shoot cultures *in vitro* and then transferred into pots and grown in a greenhouse (16 h/8 h of light/dark, 30 °C/22 °C day/night). After 2 months of growth, five plantlets per line were transferred to field in the Wushe Plantation for Transgenic Crops, Shanghai, China (31° 13′ 48.00″ N, 121° 28′ 12.00″ E) in early May for 6 months of growth. The phenotypic performance of field plants was recorded regularly until harvest and storage root parameters were analyzed.

Genomic DNA extraction and mutation analysis

Cassava genomic DNA was extracted from young leaves of in vitro shoot cultures using the Hi-DNAsecure Plant Kit (TIANGEN, Beijing, China). Four pairs of oligonucleotide primers were synthesized to detect the first to fifth exons in the *SBE2* gene (Table S1) by PCR. PCR amplification was carried using I-5™ 2X High-Fidelity Master Mix (TsingKe, Beijing, China) following the manufacturer's instructions. PCR products were purified with the TIANgel Midi Purification Kit (TIANGEN, Beijing, China) and cloned into the P-Easy-Blunt vector (TransGen Biotech, Beijing, China), about 8-16 colonies of transformants were sequenced and analyzed. Pairwise blast searches were performed to compare the sequences of the WT and *SBE2* mutants.

Protein extraction, immunoblotting and in-gel enzyme activity analysis

Soluble protein was extracted from cassava storage roots in non-denatured solvent (50 mM Tris-HCl, pH 7.5, 2 mM EDTA-2Na, 0.4 mM PMSF) on ice. After centrifuged for 10 min at 20,000×*g*, the protein was quantified by Modified Bradford Protein Assay Kit (Sango Biotech, Shanghai, China). 40 μg of protein was subjected to SDS-PAGE and blotted onto nitrocellulose filter membranes. Western blotting was performed using rabbit antiserum of SBE2 which was obtained by ABclonal Technology (Wuhan, China) using purified recombinant protein as an immune antigen.

To analyze BE enzyme activity, 40 μg of soluble protein was subjected to native-PAGE with 3.3% (w/v) stacking gel and 5% (w/v) separating gel with (Sun et al. 1996) or without 1% (w/v) (Yamanouchi and Nakamura,1992) starch from TMS60444 storage roots at 4 ℃ for 3 h as

described previously After electrophoresis, the gel was incubated in reaction buffer containing 50 mM HEPES-NaOH pH7.4, 50 mM G-1-P, 2.5 mM AMP, 10% (v/v) glycerol and 50 units rabbit muscle phosphorylase (Sigma-Aldrich, St.Louis, USA) at 30℃ overnight. The gel was stained with the I_2/KI solution until the bands occurred. To quantify protein bands from gels or films, intensity values of SBE proteins and enzyme activity were analyzed with Image J software (https://imagej.nih.gov/ij) and actin was used as the internal control.

Starch extraction and amylose granule analysis

Storage roots of 6-month-old plants harvested from the field were used for starch extraction and subsequent analysis. After washing and peeling, storage roots were homogenized thoroughly with water in a Waring blender (Waring Commercial, New Hartford, CT, USA) and then passed through a 100-mesh filter to remove impurities. When the starch completely settled, the supernatant was discarded and the starch granules were washed with distilled water several times. Then clean starch was baked in a constant temperature ventilated oven at 40 °C for 2 days and stored in a constant humidity cabinet.

Starch granule staining and light microscopy were performed as described by Bull et al. (2018) with slight modification. Ninety microliters of 20 mg/mL purified starch was mixed with 10 µL of 30% Lugol's solution and centrifuged for 1 min at 3000×*g*. After discarding the supernatant, the starch pellet was resuspended with 20 µL of 50% (v/v) sterile glycerol and observed under an Olympus microscope. The starch granule morphology was observed by scanning electron microscope (SEM) as described (Zhou et al. 2020). The granule size distribution of starch was determined using a Master-size 2000 laser diffraction instrument (Malvern Instruments Ltd., Worcestershire, UK) in wet-cell mode as previously described (Zhou et al. 2015).

Analysis of total starch, resistant starch, and amylose contents

Total starch content and resistant starch content were measured according to the AOAC's official method by using Total Starch (100 A) Kit and Resistant Starch Kit (Megazyme International Ireland Ltd. Co., Wicklow, Ireland). Ten milligrams of starches from storage roots as well as 10 mg of standard amylose/amylopectin was first mixed with 100 µL of 95% ethanol (v/v) and then 900 µL sodium hydroxide (1 M) while vortexing. The mixture was heated in a boiling water bath for 10 min, then cooled to room temperature and transferred to a 10 mL volumetric flask to make up the volume by adding H_2O. Next gradient-diluted amylose solutions with concentrations of 0, 10%, 20%, 30%, 50%, 60%, 80%, and 100% were prepared using standard amylose and amylopectin. The reaction system was brought up to 10 mL in volume with 500 µL of sample supernatant, 100 µL of 1 M acetic acid solution, 200 µL of 2% (v/v) iodine potassium iodide and double distilled water. After incubation at room temperature for 10 min, detection of amylose content was performed by measuring the absorbance at 720 nm in a Thermo Scientific Multiskan GO spectrophotometer (ThermoFisher Scientific, Vartaa, Finland).

Analysis of starch pasting and thermal properties

Starch pasting properties were analyzed by a Rapid Visco Analyzer (RVA-4, Newport Scientific, Australia). To calculate the starch dry weight, the moisture content was first measured through high heat drying using a Rapid Moisture Analyzer (HR83-P, Metter Toledo, Switzerland). Dried starch was suspended in double distilled water at a ratio of 7% (w/v) and then analyzed. The program was as follows: temperature was increased to 50 °C and held for 1 min, then increased to 95 °C at a rate of 12 °C/min and kept for 3 min. Next, the temperature was decreased to 50 °C at the same rate and maintained for 3 min. The stirring speed was constant at 160 rpm throughout the analysis except for the 960 rpm applied during the first 10 s.

The starch thermal properties were analyzed by a differential scanning calorimeter (DSC Q2000; TA Instruments Ltd., Crawley, UK). 3 mg starch was added to 9 µL distilled water in an aluminum pan and incubated at room temperature for 24 h. With an empty aluminum pan as a reference, the sample was heated at a speed of 10 °C/min from 30 to 105 °C, and the gelatinization temperature and enthalpy were determined and recorded (Universal Analysis 2000, TA Instruments Ltd., Crawley, UK).

Determination of starch branching degree, chain length distribution, and molecular weight

Starch branching degree was determined using a Bruker BioSpin GmbH NMR spectrometer equipped with a tempering unit (Fuentes et al. 2016). Purified starch (10 mg) was mixed with 1 mL of deuterated DMSO and fully dissolved at 80 °C overnight. The mixture was centrifuged at 14,000 rpm to clean out undissolved starch granular debris or impurities 600 µL of supernatant was taken and loaded into an NMR tube. The heating temperature was set at 65 °C, and scanning was performed 32 times. Data were collected and analyzed with MestReNova.

The chain length distribution was detected by high-performance anion-exchange chromatography with pulsed amperometric detection (HPAEC-PAD; Dionex-ICS 5000+; Dionex Corporation, Sunnyvale, CA, USA) as previously described (Zhou et al. 2020). Purified starch (5 mg) was deproteinized with protease, cleaned with sodium bisulfite to remove contaminated proteins or impurities in starch, and debranched with isoamylase (1000 U/μL) following the methods of Tran et al. (2011) and Li et al. (2011).

The molecular weight distribution of debranched starch was analyzed using gel permeation chromatography (U3000, Thermo, USA) differential optical (Wyatt technology, CA, USA) multi-angle laser light scattering system (Wyatt technology, CA, USA) with different columns (Ohpak SB-803/805 HQ), and the column temperature was set at 65 °C. Standard dextrans of known molecular weights (350; 3 K; 21 K; 130 K; 600 K; 820 K; and 3755 K) were used for column calibration.

X-ray diffraction analysis

X-ray diffraction analysis of the purified starch was performed using a D8 Advance Bruker X-ray diffractometer (BrukerAXS, Karlsruhe, Germany). The samples were scanned through the 2θ range of 5°–40° at a rate of 4°/min and a step size of 0.02°. The results were analyzed using Jade 5.0 software (Materials DataInc., Livermore, CA, USA).

Statistical analysis

Samples were collected from three independent plants per line and then pooled for further analyses. All statistical analysis was performed using Duncan's multiple range test or Student's *t*-test. A value of $P < 0.05$ was considered statistically significant.

Results

Efficient dual sgRNA-directed knock-out of the cassava *SBE2* gene

The cassava *SBE2* gene (GenBank accession no. MK086026.1) is 19,327 bp in length, has 22 exons, and encodes a protein of 837 amino acids. Phylogenetic analysis of cassava SBE2 and SBEs from other crops, including barley, maize, rice, wheat, potato, and sweet potato, showed evolutionary divergence of SBE proteins (Fig. S1). Among the analyzed SBE proteins, cassava SBE2 is closer to SBE2.1 and SBE2.2 from *Arabidopsis* in the SBE2 cluster; while the cassava SBE1 is classified into another cluster. The low nucleotide sequence homology between cassava *SBE1* and *SBE2* facilitated the design of *SBE2*-specific sgRNAs. Two different sgRNAs were designed to target the second exon and the fifth exon of *SBE2* to guarantee target gene editing (Fig. 1). After friable embryogenic callus (FEC)-mediated transformation using *Agrobacterium tumefaciens*, 43 transgenic cassava plant lines were recovered using hygromycin selection. These lines were further verified by PCR using two pairs of oligonucleotide primers (Supplementary Table S1) surrounding the target regions, and the PCR products were sequenced. Most of the transgenic lines had mutations in the *SBE2* gene; the mutation rate was 93.02% (40/43). These mutations including nucleotide insertions and deletions could be classified into 8 mutated lines according to their encoding sequences (Fig. 1). Homozygous mutated line 1 (M1) was a 6-bp deletion (TCCTGA) before the protospacer adjacent motif (PAM) sequence CGG, which led to a loss of proline and asparagine. Mutant line 2 (M2) was biallelic mutations in exon 2 including 1-bp insertion (A) in one allele and a 6-bp deletion (TCCTGA) in the other allele. Mutant lines 3, 4 and 5 (M3, M4 and M5, respectively) were heterozygous: M3 had 1-bp insertion (T/A) in the second and fifth exon, respectively; M4 showed a 2-bp insertion (GA) around the CGG sequence in the second exon; and M5 had a 6-bp deletion (CTGATG) and 1-bp insertion (T) in the second exon. Mutant lines 6 and 7 (M6 and M7) were homozygous mutations, showing large fragments (55 bp or 31 bp) deletion in the second exon and a 1-bp insertion (T) near the PAM sequence AGG in the fifth exon. Mutant line 8 (M8) had biallelic mutation, having an 8-bp deletion (TTCCTGAT) and a 31-bp deletion (GGT CACTGCGTCTAAAAGAGTCCTTCCTGAT) in different alleles of the second exon. Its reading frame of the fifth exon was deleted by 43 bp in one allele and no change in another allele. These results showed that mutagenesis of the *SBE2* gene in our study mainly occurred at − 3 to − 10 bp adjacent to PAM (NGG) site in M1–M5 mutant lines, but there were also large deletions encompassing the PAM sequence in M6–M8 mutant lines.

Mutation of cassava *SBE2* affects plant growth in field

To explore whether mutations in *SBE2* have an impact on growth, wild type (WT) and eight *SBE2*-mutated lines (referred to as M lines) were planted in the field for 6 months of growth. The amount of foliage produced by M lines was variable; some lines including M1-M3 showed an obvious reduction in growth in comparison with WT. The storage root phenotypes, namely root biomass, root length, root diameter, and root number (Fig. 2a–e), also differed between WT and the mutants. Compared with the 2.80 kg/plant average biomass of WT storage roots, average biomass of the mutants ranged from 0.89 to 1.93 kg/plant (Fig. 2a, b). The

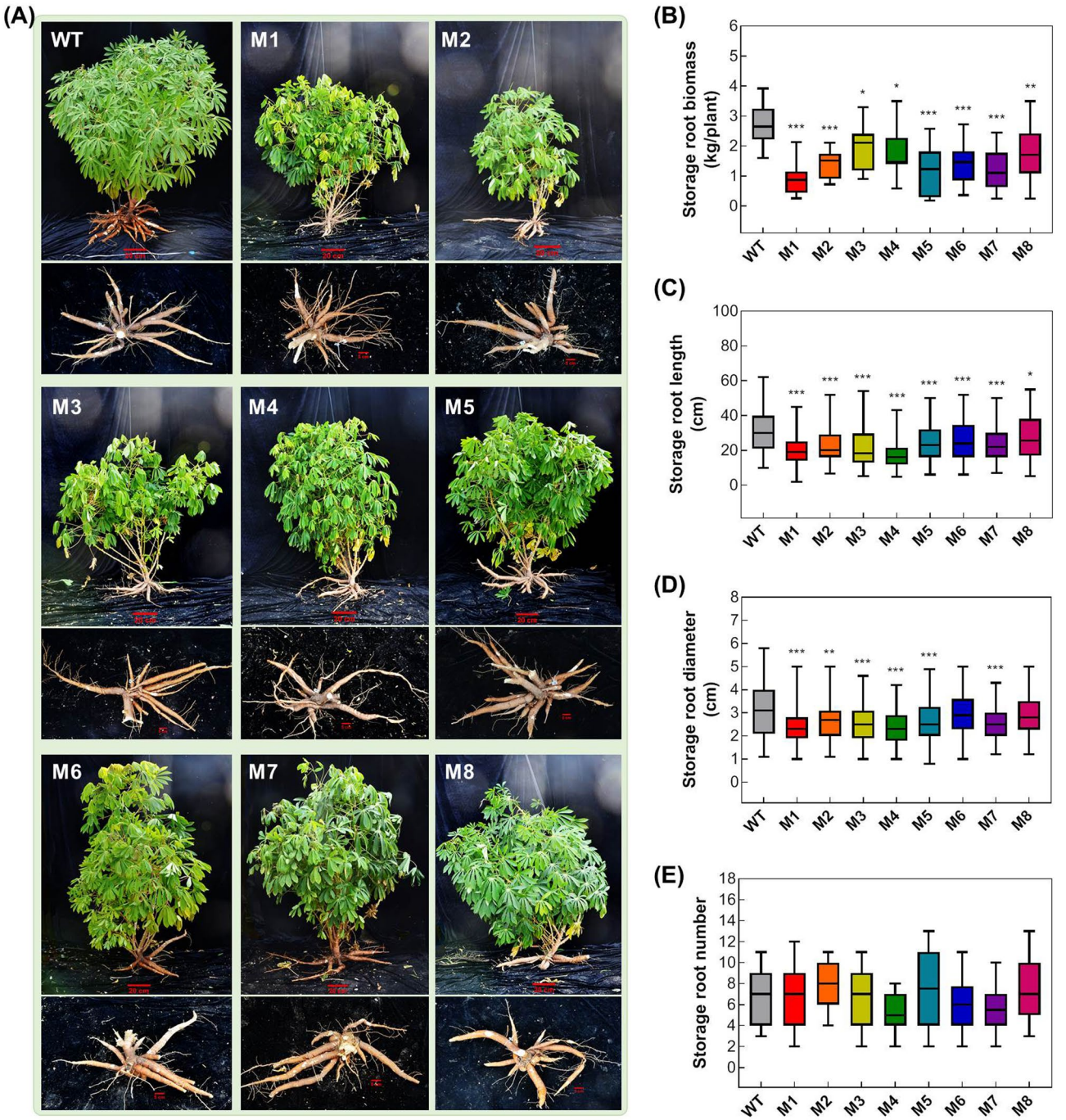

Fig. 2 Phenotypes of 6-month-old field-grown cassava plants with mutations in *SBE2*. **a** Canopy architecture (upper panel) and storage roots (lower panel) of wild-type (WT) and *SBE2*-mutated plant lines. **b–e** Comparisons of storage root biomass (**b**), storage root length (**c**), storage root diameter (**d**), and storage root number (**e**). Statistical differences were determined by Student's *t*-test; $*P < 0.05$, $**P<0.01$, $***P<0.001$

mutant roots were also shorter; the average root length of the mutants ranged from 18.00 to 28.30 cm, and that of WT was 32.20 cm (Fig. 2a, c). The average storage root diameter in WT, 3.11 cm, was slightly larger than that of the mutated lines, which ranged from 2.41 to 2.99 cm (Fig. 2a, d). The average number of storage roots was around 7–8; no significant difference was found between WT and the mutated lines (Fig. 2a, e). In general, mutations in the *SBE2* gene caused a reduction in the growth of storage roots, and the CRISPR/

Cas9-generated mutant lines resemble those produced using RNAi (Zhou et al. 2020).

SBE2-knockout mutants show higher amylose content and a lower degree of branching in starch

To verify SBE2 expression, the protein level in WT and the *sbe2* mutants was analyzed by immunodetection using total proteins extracted from 6-month-old cassava storage roots. Immunoblotting results showed that SBE2 proteins were barely detectable in M6, M7, and M8 mutant lines, while in lines M2, M3, M4 and M5, the protein levels were slightly lower or similar to those in WT when compared to the ratio between SBE2 and actin protein. Only the SBE2 protein in the homozygous M1 was higher than that of WT (Fig. 3a, left panel). Native PAGE analysis showed that the enzymatic activity of SBE2 was only absent in the M6, M7, and M8 mutant lines and detectable in other mutant lines, indicating SBE2 activity had significant changes in the large fragment-deleted mutants (Fig. 3a, right panel). Meanwhile, the enzymatic activity of SBE1 protein was not affected in all mutant lines (Supplementary Fig. S2).

The significantly higher apparent amylose content in the M6–M8 mutant lines was detected by iodine colorimetric assay. Compared with WT, which had an amylose content of 26.03%, the M6, M7, and M8 mutants had amylose contents of 41.26%, 48.34%, and 51.81%, respectively (Fig. 3b). No obvious difference was detected between WT and mutant M4. However, the amylose contents in M1, M2, M3, and M5 (around 20%) were relatively lower than that of WT (Fig. 3b). Moreover, a higher content of resistant starch was also detected in the M6 to M8 mutants, having a minimum of 15.7% more than that of WT. The resistant starch content in M1–M5 mutant lines were lower than that in WT except for M2 mutant line (Fig. 3c). The total starch content was slightly lower in M6–M8 mutant lines compared to that of WT (Supplementary Fig. S3a). After iodine staining for 5 min, the starch granules of WT and mutants M1–M5 were stained a light-blue color, while those of mutants M6–M8 were a dark-blue color (Fig. 3d), which also indicated higher amylose content in these mutants. Further ^{1}H nuclear magnetic resonance (^{1}H-NMR) analysis showed that the degrees of starch branching in M6–M8, which ranged from 1.96 to 3.01% (Table 1), were dramatically lower than those in WT (3.75%) and the other M mutants (3.38–3.75%). The results confirmed that the SBE2 protein was responsible for starch branching in cassava. Nevertheless, no obvious difference was found in the starch granule morphology among WT and *SBE2*-mutated plants, all having similar granule size distribution patterns and shapes (Supplementary Fig. S3b-d).

SBE2 mutants have variable starch pasting properties

Starch pasting profiles in the *SBE2* mutant lines were analyzed by a rapid visco analyzer (RVA). In general, the starches of mutants M1 to M5 had slightly higher peak viscosity (PV), hot paste viscosity (HPV), cold paste viscosity (CPV), and peak time and lower pasting temperature (PT) in comparison with WT starch. In contrast, starches of mutants M6 to M8 had significantly higher HPV, CPV, PT, and peak time, but dramatically lower breakdown (BD) values. These findings indicated that the high amylose starch in M6 to M8 might be easier for their retrogradation than that of WT. HPV values, reflecting the resistance to shear thinning, of starch from all mutants were higher compared with that of WT. In particular, the starches from M6 to M8 had HPV values ranging from 1809 to 2255 cP, which were two-fold higher that of WT (895 cP). The peak times (ranging from 5.80 to 7.00) and PTs (ranging from 71.58 to 82.10 °C) of the starches in M6 to M8 were all higher than those of WT, indicating slower gelatinization of these starches (Fig. 4a; Table 2).

Thermal analysis of storage starch showed that higher temperatures were required for melting M6 to M8 starches compared with WT starch, but that lower temperatures were required for melting the M1 to M5 starches. The onset temperature (T_o) and top melting temperature (T_p) for WT starch were 56.47 and 59.59 °C, respectively. These parameters are significantly higher for the starches of the M6, M7, and M8 mutants, which had T_o/T_p values of 60.61/67.85 °C, 60.90/66.26 °C, and 60.88/66.65 °C, respectively. There were no significant differences in the conclusion temperature (T_c) and the enthalpy (ΔH) among WT and all the mutant lines (Table 3). The increased T_o and T_p showed that the starches from the M6, M7, and M8 mutants were more difficult to gelatinize compared with those of WT and the M1–M5 mutant lines (Fig. 4b; Table 3).

SBE2 determines fine structure of amylopectin and thus affects the semi-crystallinity property of storage starch

The native storage starch of WT cassava has typical A-type crystals with 1 doublet around 17° (2θ) and 2 singlets around 15° and 23° (2θ) in X-ray diffraction (XRD) spectra (Defloor et al. 1998; Zhao et al. 2011; Zhou et al. 2020). In contrast to WT starch, the starches from the M6, M7, and M8 mutants showed the typical patterns of B-type crystallinity, showing diffractograms with additional singlets at 5° (2θ) and 20° (2θ), doublets replacing the singlets at 23° (2θ), and singlets substituting for doublets at 17° (2θ). For the starches of the M1 to M5 mutants, a transitional stage from A- to B-type crystallinity was observed, with starches showing additional

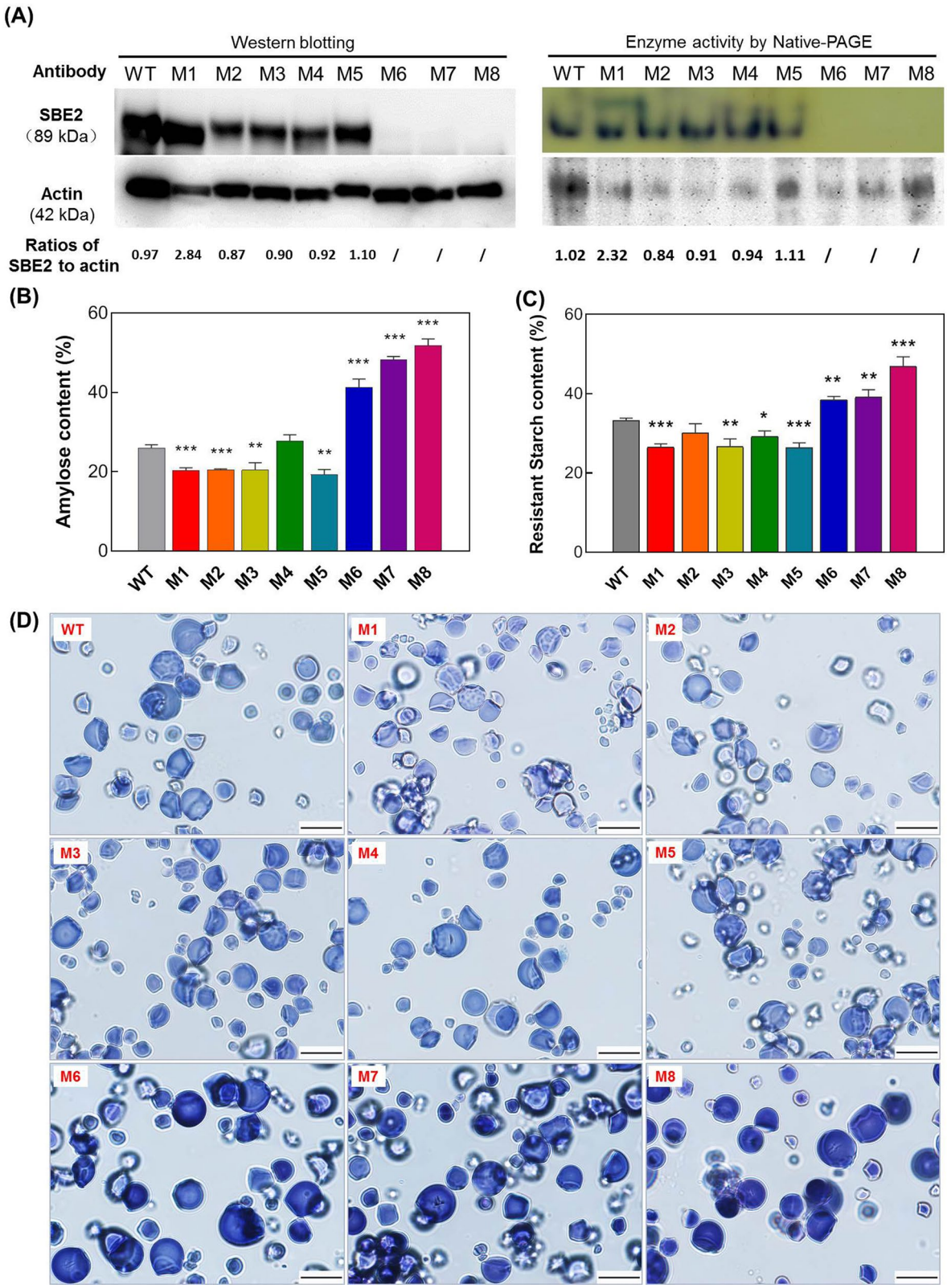

small peaks at 5° (2θ) and singlets substituting for doublets at 17° (2θ). These peak intensities were weaker than those of WT at 23° (2θ). The results indicated that the starches of *SBE2* mutants displayed different crystallinity types in comparison with those of WT (Fig. 5).

◂**Fig. 3** SBE2 protein detection and starch characteristics of *SBE2*-mutated cassava. **a** Immunodetection and in-gel enzyme activity of SBE2 in total proteins extracted from storage roots of wild-type (WT) and *SBE2*-mutated cassava plants. Actin protein was used as the control. The method was used as described previously (Yamanouchi and Nakamura 1992). **b-c** Amylose content (**b**) by iodine colorimetric assay and resistant starch content (**c**) in the storage roots. Error bars are means ± SD ($n = 3$). Statistical differences were determined by Student's *t*-test; $*P < 0.05$, $**P<0.01$, $***P<0.001$. **d** Light microscopy of iodine-stained purified starch granules of WT and *SBE2*-mutated cassava lines. Bar = 10 µm

To investigate the effect of *SBE2* mutations on amylopectin structure, the chain length distribution was measured by high performance anion exchange chromatography-pulsed amperometric detection (HPAEC-PAD). Starches from the M1 to M5 lines showed a slight decrease in short and medium chains (degree of polymerization [DP] values 6–13 and 20–39, respectively), and an increase in long chains (DP 40–60) compared with WT. For lines M6 to M8, notably fewer chains with DP 6–13 and more chains with DP 25–70 were detected (Fig. 6). According to the branching fractions of amylopectin, it revealed that starches from M6, M7, and M8 had fewer short chains and more long chains in amylopectin than those of lines M1 to M5. Nevertheless, no significant change of starch granule size was found among all the mutations compared with WT (Supplementary Fig. S3b, c).

Branching characteristics of these starches were also measured by molecular weight distribution analysis using gel permeation chromatography (GPC). In GPC analysis, there are three peaks, peak1, peak2, and peak3, which represent amylopectin with short-branch chains, amylopectin with long-branch chains, and amylose molecular, respectively (Song and Jane, 2000). The ratio of the areas of peak1 to peak2 reflects the branching pattern of amylopectin (Wang et al. 1993). The M6-M8 mutant lines had higher peak2 and peak3 ratios (Fig. 7; Table 4), which showed that M6-M8 mutant lines possessed prominently more amylopectin long-chain (29.19%-34.28%) and amylose chain (19.65–28.87%) compared with WT (21.21% and 13.98%, respectively).The results was consistent with the apparent amylose content estimated by colorimetric assay (Fig. 3b).

Discussion

Breeding high-amylose cassava is considered one of the most important goals in cassava breeding programs to meet the increased demand for potential applications in starch industries. Although the generation of high-amylose cassava has recently been accomplished by the knockdown of cassava branching enzyme genes using RNAi technology (Zhou et al. 2020), direct mutagenesis of the *SBE2* gene by CRISPR/Cas9 system provides a practical approach for developing transgene-free cassava through further hybridization in future. Several reports have demonstrated the feasibility of site-specific gene editing in cassava using the CRISPR/Cas9 technique to improve traits including waxy starch and disease resistance (Odipio et al. 2017; Bull et al. 2018; Gomez et al. 2019). The function of the cassava *SBE2* gene in amylopectin synthesis in storage roots was previously validated (Zhou et al. 2020), and here high-amylose cassava was further successfully developed using CRISPR/Cas9-mediated *SBE2* editing; the storage roots of the *sbe2* mutants had amylose contents higher than 50% (Fig. 3b). Their resistant starch contents were also increased, showing a positive correlation with high amylose starch content (Cai et al.2015; Zhou et al. 2016). Furthermore, these *sbe2* mutants will provide an invaluable resource for studying the protein-protein interactions and starch biosynthetic protein complex in storage roots of root crops, as did in cereal endosperms (Tetlow et al. 2015).

Mutations generated by CRISPR/Cas9 editing of plant genomes are variable, and include nucleotide- and fragment-based mutations around the PAM region (Li et al. 2018). In the *SBE2* mutants, nucleotide insertions and short- or long-fragment deletions in the *SBE2* gene were identified (Fig. 1). Although two sgRNA target sites for *SBE2* were used in our study, a mutation preference was noticed. The target in exon 2 of *SBE2* was more frequently mutated compared with that in exon 5. This might be due to the difference of editing efficiency and specificity of the sgRNA (Liang et al. 2016). At the protein level, complete depletion of SBE2 protein was only observed in the homozygous mutants M6, M7, and biallelic mutant M8, which had long-fragment deletions in *SBE2* (Figs. 1 and 3a). In these mutants, loss of SBE2 was associated with a dramatic increase of amylose-content and reduced degree of branching in starch, confirming that SBE2 mainly functions in amylopectin branching (Fig. 3b). Other *SBE2*-edited mutants, either biallelic or heterozygous, showed expression of SBE2 protein but their amylose starch contents were slight lower than that of WT, possible due to the decreased SBE2 protein levels or the disruption of SBE2-SSI/SSII interactions, since the SBE2-SSI/SSI interaction is essential for organizing the starch biosynthetic enzyme complex in starch biosynthesis (He et al. 2020; Teltow et al. 2015). This also explains the phenotype changes with delayed plant growth in these *sbe2* mutants, as evidenced in other crops (Hofvander et al. 2004). So far, CRISPR/Cas9-mediated *SBE2* editing in rice, potato and sweet potato has been successfully reported for high-amylose trait improvement (Sun et al. 2017; Wang et al. 2019; Zhao et al. 2021).

Most plant species with high amylose content, especially in endosperms of cereals, may have smaller granules and more irregular morphologies, depending on the levels of amylose content. Simultaneously suppressing all SBEs

Table 1 Degree of starch branching in *SBE2*-mutated cassava detected by ^{1}H NMR

Cassava line	Area1	Area2	Degree of branching(%)
WT	360,462	13,993	3.75
M1	903,003	32,009	3.38
M2	929,642	36,689	3.75
M3	1,077,584	42,300	3.75
M4	970,116	33,957	3.38
M5	787,585	31,081	3.75
M6	794,693	24,458	3.01
M7	793,308	20,305	2.53
M8	561,845	11,439	1.96

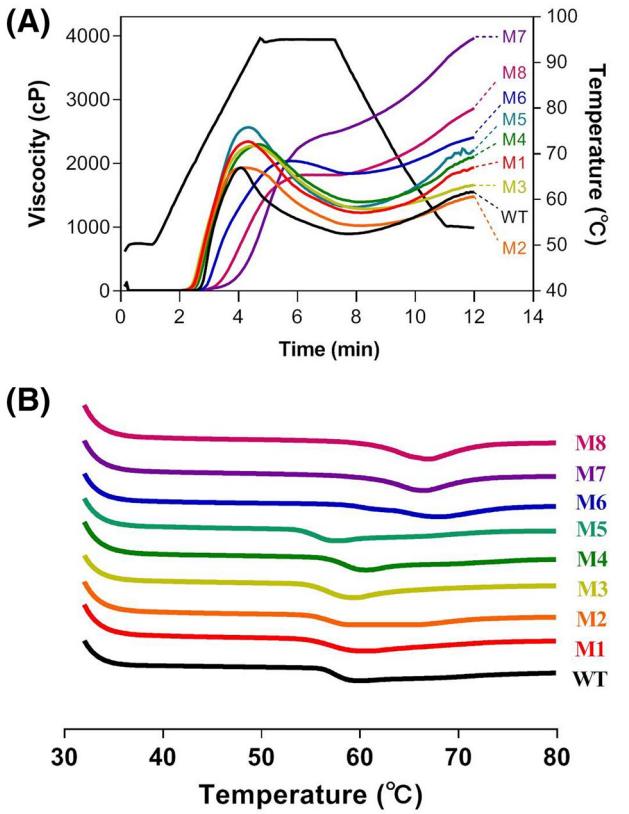

Fig. 4 Pasting and thermal profiles of S*BE2*-mutated cassava starches. **a** Pasting profiles of storage starches analyzed by a Rapid Visco Analyzer. Starches were isolated from storage roots of wild-type (WT) and *SBE2*-mutated cassava plants. Starch samples were prepared as a 7% (w/v) starch suspension. **b** Differential scanning calorimeter thermograms of storage starches from WT and *SBE2*-mutated cassava plants. Samples were prepared using dried starch powder

(SBE I, SBE IIa, SBE IIb) in barley could lead to irregular shapes of starch granules (Carciofi et al. 2012), and such change was also found in potato lines with both reduction of SBE1and SBE2 (Tuncel et al. 2019). In root crops such as cassava and sweet potato, even though amylose content increases up to 60%, their starch granule shapes did not changes significantly in comparison with normal starches that have 20-30% amylose (Zhou et al. 2015). In this study, the apparent amylose content is less than 60% and their granule size and morphology did not detect significant changes as evidenced by granule size distribution and SEM analysis (Figs. 3b, S3d). Based on a recent study using waxy and high-amylose sweet potato starch (Zhang et al. 2019), the formation of new semicrystalline lamellae (named Type II) in starch in addition to the widely reported Type I lamellae has been revealed in sweet potato that had either downregulated GBSSI (for waxy starch) or SBE (for high-amylose starch) activity. Such lamellae changes might support the structure flexibility in starch.

Meanwhile physico-chemical properties of cassava starches from the M6 to M8 lines also resembled those of mutants generated using RNAi approaches. Consistent with the starches from *SBE2*-RNAi transgenic plants, the M6 to M8 mutants had significantly higher values of HPV, CPV, PT, and peak time, but a lower BD value, indicating a higher capacity for resistance to shear thinning and a slower gelatinization process (Fig. 4a; Table 2). Several reports indicated that there is positive correlation between amylose content, resistant starch, and gelatinization temperature (Park et al. 2007; Chung et al. 2011; Cai et al. 2015). Indeed, our results were consistent with previous reports in sweet potato and cassava (Zhou et al. 2015; Zhou et al. 2020), showing a higher temperature during the melting process in these high-amylose cassava starches. The transition from an A-type to B-type crystallinity pattern among these starches was also observed in starches with increased amylose content isolated from *SBE2*-RNAi sweet potato and cassava (Zhou et al. 2015; Zhou et al. 2020); these starches showed significant changes at 5° (2θ), 17° (2θ), 20° (2θ) and 23° (2θ) in X-ray diffractograms (Fig. 5). Since amylose content affects the physical-chemical properties of starch and determines the potential for application in the starch industry (Zhou et al. 2015), our study provides techniques for cassava genetic improvement and useful material for functional exploration.

Amylopectin chain profiles are determined by the activity of SBEs (Testerm et al. 2004). In cereals, SBEI and SBEII are mainly responsible for catalyzing the formation of branch points (Guan and Preiss, 1993). In rice, amylopectin

Table 2 Viscosity properties of storage starches in *SBE2*-mutated cassava

	Peak viscosity (cP)	Hot paste viscosity (cP)	Breakdown (cP)	Cold paste viscosity (cP)	Setback (cP)	Peak time (min)	Pasting temperature (℃)
WT	1933 ± 25.87c	895 ± 19.86f	1038 ± 10.07b	1566 ± 264e	671 ± 248 cd	4.07 ± 0.00f	69.57 ± 0.58d
M1	2345 ± 24.70ab	1227 ± 27.61d	1119 ± 28.10a	1937 ± 52.05d	710 ± 72.81 cd	4.31 ± 0.03e	66.22 ± 0.06f
M2	1935 ± 12.70c	1024 ± 15.04e	910 ± 2.52c	1544 ± 27.40f	520 ± 42.36e	4.15 ± 0.04f	66.98 ± 0.03e
M3	2276 ± 64.38b	1285 ± 20.65 cd	991 ± 54.67bc	1698 ± 15.10e	413 ± 22.55e	4.49 ± 0.03d	65.32 ± 0.08 g
M4	2301 ± 20.81b	1394 ± 53.56c	907 ± 37.04c	2160 ± 118c	766 ± 167 cd	4.67 ± 0.00c	67.52 ± 0.49d
M5	2568 ± 70.87a	1312 ± 10.07 cd	1255 ± 63.52a	2144 ± 35.30c	832 ± 45.13c	4.31 ± 0.03e	65.83 ± 0.46f
M6	2042 ± 39.00c	1842 ± 28.75b	200 ± 20.07d	2477 ± 36.43c	635 ± 13.32d	5.80 ± 0.13b	71.58 ± 0.42c
M7	2462 ± 73.76a	2255 ± 97.81a	207 ± 48.05d	4134 ± 259a	1879 ± 163a	7.00 ± 0.00a	82.10 ± 1.00a
M8	1827 ± 22.27d	1809 ± 17.09b	18.0 ± 7.21e	3048 ± 10.44b	1239 ± 27.18b	6.60 ± 0.42a	76.47 ± 0.40b

Table 3 Thermal properties of *SBE2*-mutated cassava determined by a differential scanning calorimeter

Cassava line	T_o (℃)	T_p (℃)	T_c (℃)	ΔH (J/g)
WT	56.47 ± 0.14b	59.59 ± 0.08b	73.34 ± 0.18c	13.58 ± 0.41a
M1	54.77 ± 0.17c	59.82 ± 0.25b	73.79 ± 0.18c	13.60 ± 0.46a
M2	54.95 ± 0.15c	58.87 ± 0.23c	72.91 ± 0.61d	13.11 ± 0.85a
M3	54.70 ± 0.07c	58.95 ± 0.06c	68.92 ± 1.00e	13.16 ± 0.93a
M4	56.57 ± 0.16b	60.13 ± 0.32b	77.53 ± 0.63a	13.10 ± 1.17a
M5	53.97 ± 0.11d	57.34 ± 0.23d	73.08 ± 0.45c	13.01 ± 1.02a
M6	60.61 ± 0.13a	67.85 ± 0.65a	75.40 ± 0.17b	12.64 ± 0.92a
M7	60.90 ± 0.24a	66.26 ± 0.44a	72.46 ± 0.35d	12.13 ± 1.41a
M8	60.88 ± 0.07a	66.65 ± 0.16a	73.01 ± 0.09d	13.69 ± 1.29a

from endosperm of the *sbe1* mutant had fewer long chains with DP ≥ 37 and chains with DP 12–21 (Satoh et al. 2003). Cereal SBEII isoforms SBEIIa and SBEIIb have distinct expression patterns; SBEIIa is ubiquitously expressed in all tissues and SBEIIb is specifically present in the endosperm (Nishi et al. 2001). In general, SBEIIb enzymes play a specific role in the formation of short chains of amylopectin, and the *amylose extender* (*ae*) of maize, in which the gene encoding SBEIIb is mutated, has a high amylose starch phenotype (Nishi et al. 2001). Like *SBE2*-RNAi cassava, *SBE2*-knockout cassava lines showed high-amylose phenotypes with higher levels of glucan chains around DP 25–70 but lower levels of glucan chains with DP 10–25 in starch granules, indicating that cassava SBE2 mainly functions in the formation of the short chains of amylopectin in storage roots, especially those with DP<25 (Fig. 6). This also indicates that other SBE isoforms are required for long-chain biosynthesis in cassava, as another SBE gene *SBE1* have been identified based on blast searches of the genome sequence (Pei et al. 2015). The higher levels of glucan chains with DP>40 in starches of the *sbe2* cassava mutant may cause the formation of more solid, double-helical crystallinities in amylopectin molecules, leading to an increase in the thermal parameters T_o and T_p, and transformation of starch

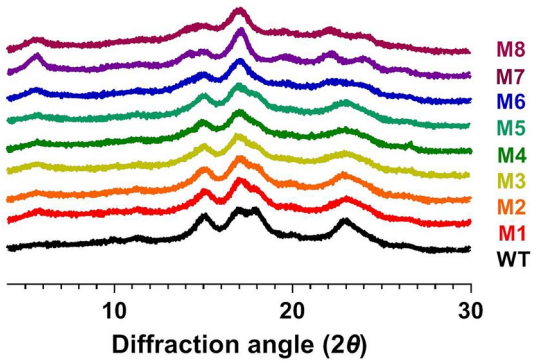

Fig. 5 X-ray diffractograms of *SBE2*-mutated cassava starches. Starches were isolated from storage roots of wild-type (WT) and *SBE2*-mutated cassava plants. Samples were prepared using dried starch powder

granules with an A-type X-ray diffraction pattern to those with a B-type pattern (Figs. 4b and 5; Table 3), as reported for other high-amylose starches in species including rice, wheat, cassava, potato, and sweet potato (Jane et al. 1999; Zhou et al. 2015; Zhou et al. 2020).

In conclusion, our study reports the generation of high-amylose cassava with increased resistant starch by CRISPR/

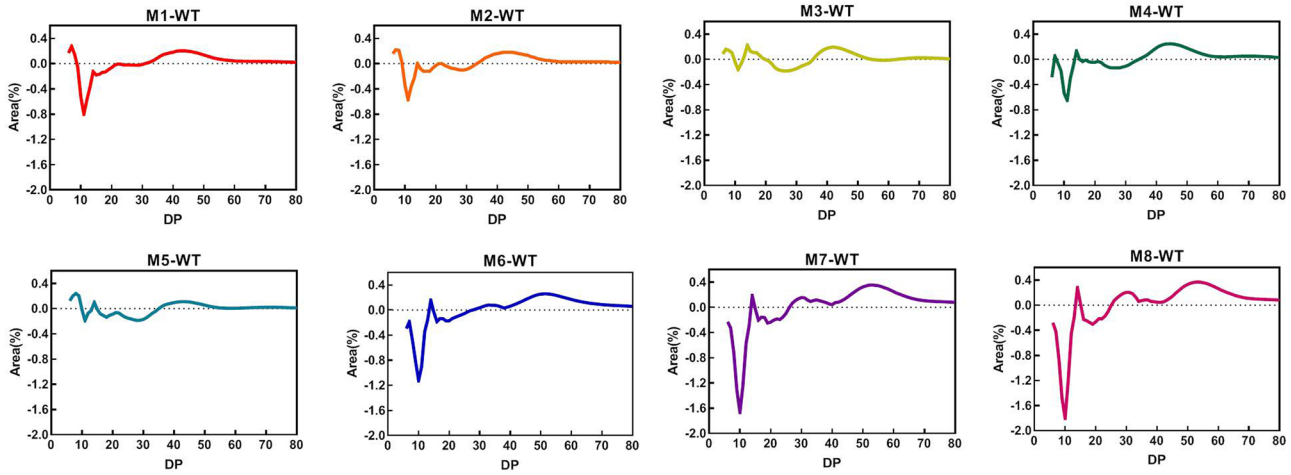

Fig. 6 Comparisons of amylopectin chain length distribution in wild-type and *SBE2*-mutated cassava starches. Differences in the chain length distribution between the wild type (WT) and *SBE2*-mutated lines were calculated by subtracting normalized CLD value for WT from that of each mutated line

Table 4 Gel permeation chromatography (GPC) parameters of storage starches in *SBE2*-mutated cassava

Starch	GPC peak area(%)			Peak 1/Peak 2
	Peak 1	Peak 2	Peak 3	
WT	64.82	21.21	13.98	3.06
M1	52.19	31.95	15.86	1.63
M2	59.74	28.81	11.45	2.07
M3	56.33	35.41	8.26	1.59
M4	64.05	23.93	12.02	2.68
M5	52.83	31.33	15.84	1.69
M6	50.34	30.01	19.65	1.68
M7	38.88	34.28	26.84	1.13
M8	41.94	29.19	28.87	1.44

Cas9-mediated mutagenesis of the *SBE2* gene, which provides a genetic resource to enrich cassava germplasm in addition to the waxy cassava produced by editing *GBSSI* and *PTST1* (Bull et al. 2018). High-amylose cassava starch showed altered starch physico-chemical properties, including pasting and gelatinization properties, chain length distribution, and crystallinity. These high-amylose cassava starches with different properties can be used in specific industrial fields. The novel materials produced in this study could be used as parents through proper selfing or intermating hybridization between different transgenic lines to segregate the trait and to eliminate Cas-9 gene in progenies, generating plants without foreign genes.

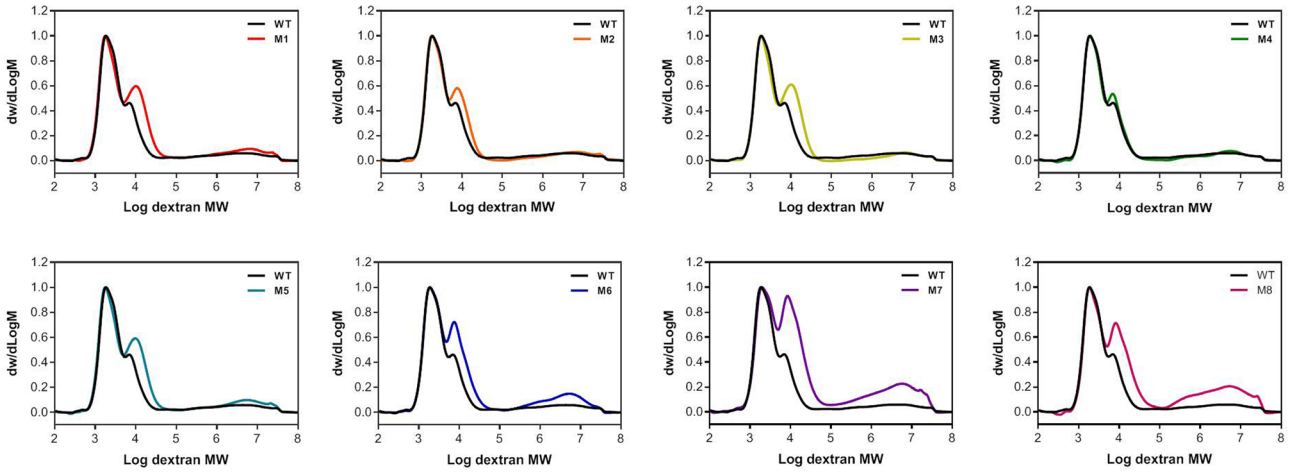

Fig. 7 Gel permeation chromatography profiles of *SBE2*-mutated cassava. Starches from storage roots of wild-type (WT) and *SBE2*-mutated plants were debranched by isoamylase treatment before gel permeation chromatography detection

Supplementary Information The online version contains supplementary material available at https://doi.org/10.1007/s11103-021-01215-y.

Acknowledgements We thank Nan Yang and Fuchao Shi for assistance in vector construction and starch properties analysis. This work was supported by grants from the National Key R&D Program of China "Efficient Breeding Technology and Variety Creation of Tropical Crops" (2018YFD1000500), the National Natural Science Foundation of China (31871682, 32072118, 31801417), Natural Science Foundation of Shanghai (17ZR1435200), the Science and Technology Program of Guangxi (Guike-AD1850003), and China Agriculture Research System (CARS-11).

Author contribution SL performed most of the experiments and analyses and wrote the manuscript; YZ and WZ performed chain length distribution, molecular weight and NMR analyses; JJ assisted starch extraction and pasting properties measurement. XL maintained transgenic cassava; ZW and YT contributed to part of the field experiment. QM and PZ conceived and designed the study, analyzed the data and revised the paper with input from other authors. All authors discussed the results and approved the manuscript.

Declarations

Conflict of interest The authors declare no conflict of interest.

References

Andersson M, Turesson H, Nicolia A, FÓ"lt A, Samuelsson M, Hofvander P (2017) Efficient targeted multiallelic mutagenesis in tetraploid potato (*Solanum tuberosum*) by transient CRISPR-Cas9 expression in protoplasts. Plant Cell Rep 36:117–128

Bailey TL, Boden M, Buske FA, Frith M, Grant CE, Clementi L, Ren J et al (2009) MEME SUITE: tools for motif discovery and searching. Nucleic Acids Res 37:W202–8

Breuninger WF, Piyachomkwan K, Sriroth K (2009) Tapioca/cassava starch: production and use. *In : Whistler R (ed) Starch: Chemistry and technology*. Elsevier, Inc., New York, pp 541–568

Bull SE, Seung D, Chanez C, Mehta D, Kuon JE, Truernit E, Hochmuth A et al (2018) Accelerated ex situ breeding of GBSS-and PTST1-edited cassava for modified starch. Sci Adv 4:eaat6086

Cai J, Man J, Huang J, Liu Q, Wei W, Wei C (2015) Relationship between structure and functional properties of normal rice starches with different amylose contents. Carbohydr Polym 125:35–44

Carciofi M, Blennow A, Jensen SL, Shaik SS, Henriksen A, Buléon A, Holm PB, Hebelstrup KH (2012) Concerted suppression of all starch branching enzyme genes in barley produces amylose-only starch granules. BMC Plant Biol 12(223):1–16

Ceballos H, Sánchez T, Morante N, Fregene M, Dufour D, Smith AM, Denyer K et al (2007) Discovery of an amylose-free starch mutant in cassava (*Manihot esculenta* Crantz). J Agric Food Chem 55:7469–7476

Ceballos H, Okogbenin E, Pérez JC, López-Valle LAB, Debouck D (2010) Cassava root and tuber crops. Handbook of plant breeding. Springer, New York

Ceballos H, Rojanaridpiched C, Phumichai C, Becerra LA, Kittipadakul P, Iglesias C, Gracen VE (2020) Excellence in cassava breeding: Perspectives for the future. Crop Breed Genet Genom 2:e200008

Chen K, Wang Y, Zhang R, Zhang H, Gao C (2019) CRISPR/Cas genome editing and precision plant breeding in agriculture. Annual Rev Plant Biol 70:667–697

Chung HJ, Liu Q, Lee L, Wei D (2011) Relationship between the structure, physicochemical properties and in vitro digestibility of rice starches with different amylose contents. Food Hydrocolloid 25:968–975

Cong L, Ran FA, Cox D, Lin S, Barretto R, Habib N, Hsu PD, Wu X, Jiang W, Marraffini LA et al (2013) Multiplex genome engineering using CRISPR/Cas systems. Science 339:819–823

Defloor I, Dehing I, Delcour JA (1998) Physico-chemical properties of cassava starch. Starch-Stärke 50:58–64

Dong L, Qi X, Zhu J, Liu C, Zhang X, Cheng B, Mao L et al (2019) Supersweet and waxy: meeting the diverse demands for specialty maize by genome editing. Plant Biotechnol J 17:1853–1855

FAO (2019) Food Outlook - Biannual Report on Global Food Markets. Rome. Licence: CC BY-NC-SA 3.0 IGO

Fuentes C, Zielke C, Prakash M, Kumar P, Penarrieta JM, Eliasson AC, Nilsson L (2016) The effect of baking and enzymatic treatment on the structural properties of wheat starch. Food Chem 213:768–774

Gomez MA, Daniel Lin Z, Moll T, Chauhan RD, Hayden L, Renninger K, Beyene G et al (2019) Simultaneous CRISPR/Cas9-mediated editing of cassava *eIF4E* isoforms *nCBP-1* and *nCBP-2* reduces cassava brown streak disease symptom severity and incidence. Plant Biotechnol J 17:421–434

Guan HP, Preiss J (1993) Differentiation of the properties of the branching isozymes from maize (*Zea mays*). Plant Physiol 102:1269–1273

He S, Hao X, Wang S, Zhou W, Ma Q, Lu X, Chen L, Zhang P (2020) MeSSII interplays the amylose and amylopectin biosynthesis by protein interactions in cassava storage root. bioRxiv doi. https://www.biorxiv.org/content/ https://doi.org/10.1101/2020.03.25.006957v2.full.pdf

Hofvander P, Andersson M, Larsson CT et al (2004) Field performance and starch characteristics of high-amylose potatoes obtained by antisense gene targeting of two branching enzymes. Plant Biotechnol J 2:311–320

Jane J, Chen YY, Lee LF, Mcpherson AE, Wong KS, Radosavljevic M, Kasemsuwan T (1999) Effects of amylopectin branch chain length and amylose content on the gelatinization and pasting properties of starch. Cereal Chem 76:629–637

Johansen IE, Liu Y, Jørgensen B, Bennet EP, Nielsen KL, Blennow A, Petersen BL (2019) High efficacy full allelic CRISPR/Cas9 gene editing in tetraploid potato. Sci Rep 9:17715

Li E, Hasjim J, Dhital S, Godwin ID, Gilbert RG (2011) Effect of a gibberellin-biosynthesis inhibitor treatment on the physicochemical properties of sorghum starch. J Cereal Sci 53:328–334

Li H, Gidley MJ, Dhital S (2019) High-amylose starches to bridge the "fiber gap": Development, structure, and nutritional functionality. Compr Rev Food Sci Food Saf 18:362–379

Li J, Manghwar H, Sun L, Wang P, Wang G, Sheng H, Zhang J et al (2018) Whole genome sequencing reveals rare off-target mutations and considerable inherent genetic or/and somaclonal variations in CRISPR/Cas9-edited cotton plants. Plant Biotechnol J 17:858–868

Li J, Jiao G, Sun Y, Chen J, Zhong Y, Yan L, Jiang D et al (2020) Modification of starch composition, structure and properties through editing of *TaSBEIIa* in both winter and spring wheat varieties by CRISPR/Cas9. Plant Biotechnol J 19:937–951

Liang G, Zhang H, Lou D, Yu D (2016) Selection of highly efficient sgRNAs for CRISPR/Cas9-based plant genome editing. Sci Rep 6:1–8

Mao Y, Zhang H, Xu N, Zhang B, Gou F, Zhu JK (2013) Application of the CRISPR–Cas system for efficient genome engineering in plants. Mol Plant 6:2008–2011

Nishi A, Nakamura Y, Tanaka N, Satoh H (2001) Biochemical and genetic analysis of the effects of amylose-extender mutation in rice endosperm. Plant Physiol 127:459–472

Odipio J, Alicai T, Ingelbrecht I, Nusinow DA, Bart R, Taylor NJ (2017) Efficient CRISPR/Cas9 genome editing of *phytoene desaturase* in cassava. Front Plant Sci 8:1780

Park IM, Ibáñez AM, Zhang F, Shoemaker CF (2007) Gelatinization and pasting properties of waxy and non-waxy rice starches. Starch 59:388–396

Pei J, Wang H, Xia Z, Liu C, Chen X, Ma P, Lu C et al (2015) Phylogeny and expression pattern of starch branching enzyme family genes in cassava (*Manihot esculenta* Crantz) under diverse environments. Mol Cell Biochem 406:273–284

Pootakham W, Shearman JR, Ruangareerate P, Sonthirod C, Sangsrakru D, Jomchai N, Yoocha T et al (2014) Large-Scale SNP Discovery through RNA sequencing and SNP genotyping by targeted enrichment sequencing in cassava (*Manihot esculenta* Crantz). PLoS ONE 9:116028

Sayre R, Beeching JR, Cahoon EB, Egesi C, Fauquet C, Fellman J, Fregene M et al (2011) The BioCassava plus program: Biofortification of cassava for sub-Saharan Africa. Annual Rev Plant Biol 62:251–272

Satoh H, Nishi A, Yamashita K, Takemoto Y, Tanaka Y, Hosaka Y et al (2003) Starch-branching enzyme I-deficient mutation specifically affects the structure and properties of starch in rice endosperm. Plant Physiol 133:1111–1121

Seung D, Soyk S, Coiro M, Maier BA, Eicke S, Zeeman SC (2015) PROTEIN TARGETING TO STARCH is required for localising GRANULE-BOUND STARCH SYNTHASE to starch granules and for normal amylose synthesis in *Arabidopsis*. PLoS Biol 13:e1002080

Song Y, Jane J (2000) Characterization of barley starches of waxy, normal, and high amylose varieties. Carbohydr Polym 41:365–377

Sun Y, Jiao G, Liu Z, Zhang X, Li J, Guo X, Du W et al (2017) Generation of high-amylose rice through CRISPR/Cas9-mediated targeted mutagenesis of starch branching enzymes. Front Plant Sci 8:298

Tetlow IJ, Liu F, Emes MJ (2015) Protein-protein interactions during starch biosynthesis. Starch. Springer, Tokyo, pp 291–313

Testerm RF, Karkalas J, Qi X (2004) Starch-composition, fine structure and architecture. J Cereal Sci 39:151–165

Tuncel A, Corbin KR, Ahn-Jarvis J, Harris S, Hawkins E, Smedley MA, Harwood W et al (2019) Cas9-mediated mutagenesis of potato starch branching enzymes generates a range of tuber starch phenotypes. Plant Biotechnol J 17:2259–2271

Tran TTB, Shelat KJ, Tang D, Li E, Gilbert RG, Hasjim J (2011) Milling of rice grains. The degradation on three structural levels of starch in rice flour can be independently controlled during grinding. J Agric Food Chem 59:3964–3973

Wang H, Wu Y, Zhang Y, Yang J, Fan W, Zhang H, Zhao S et al (2019) CRISPR/Cas9-based mutagenesis of starch biosynthetic genes in sweet potato (*Ipomoea Batatas*) for the improvement of starch quality. Int J Mol Sci 20:4702

Wang YJ, White P, Pollak L, Jane J (1993) Characterization of starch structures of 17 maize endosperm mutant genotypes with Oh43 inbred line background. Cereal Chem 70:171–179

Yamanouchi H, Nakamura Y (1992) Organ specificity of isoforms of starch branching enzyme (Q-enzyme) in rice. Plant Cell Physiol 33:985–991

Yang Z, Wang Y, Xu S, Xu C, Yan C (2013) Molecular evolution and functional divergence of soluble starch synthase genes in cassava (*Manihot esculenta* Crantz). Evol Bioinform 9:239–249

Zeng D, Liu T, Ma X, Wang B, Zheng Z, Zhang Y, Xie X et al (2020) Quantitative regulation of Waxy expression by CRISPR/Cas9-based promoter and 5'UTR-intron editing improves grain quality in rice. Plant Biotechnol J 18:2385–2387

Zhang B, Zhou W, Qiao D, Zhang P, Zhao S, Zhang L, Xie F (2019) Changes in nanoscale chain assembly in sweet potato starch lamellae by downregulation of biosynthesis enzymes. J Agric Food Chem 67:6302–6312

Zhang P, Potrykus I, Puonti-Kaerlas J (2000) Efficient production of transgenic cassava using negative and positive selection. Transgenic Res 9:405–415

Zhao X, Jayarathna S, Turesson H, Flt AS, Nestor G, González MN, Olsson N, Beganovic M, Hofvander P, Andersson R (2021) Amylose starch with no detectable branching developed through DNA-free CRISPR-Cas9 mediated mutagenesis of two starch branching enzymes in potato. Sci Rep 11:4311

Zhao S, Dufour D, Sanchez T, Ceballos H, Zhang P (2011) Development of waxy cassava with different biological and physicochemical characteristics of starches for industrial applications. Biotechnol Bioeng 108:1925–1935

Zhou H, Wang L, Liu G, Meng X, Jing Y, Shu X, Kong XL et al (2016) Critical roles of soluble starch synthase SSIIIa and granule-bound starch synthaseWaxy in synthesizing resistant starch in rice. Proc Natl Acad Sci USA 113:12844–12849

Zhou W, Yang J, Hong Y, Liu G, Zheng J, Gu Z, Zhang P (2015) Impact of amylose content on starch physicochemical properties in transgenic sweet potato. Carbohyd Polm 122:417–427

Zhou W, Zhao S, He S, Ma Q, Lu X, Hao X, Wang H et al (2020) Production of very-high-amylose cassava by post transcriptional silencing of branching enzyme genes. J Integr Plant Biol 62:832–846